

# Numerical Analysis of Flow Through and Calibration of Subsonic Open Wind Tunnel Test Section at Different Inlet Velocities

**Mari Prabu Govindan,**

Lecturer, St. Theresa International College, Thailand

**Praveen Shaju Chelladhurai,**

Lecturer, ST. Theresa International College, Thailand

## **Abstract:**

Design and analysis of subsonic open wind tunnel by using Computational Fluid Dynamics at different inlet velocities is carried out in this paper. The governing equations of fluid flow were solved numerically to calibrate the wind tunnel using computational fluid dynamics method by considering the flow as steady, incompressible, turbulent and three dimensional. To obtain a robust numerical simulation, coupled algorithm is used for pressure-velocity coupling with second order and second order spatial discretization to solve all the governing equations involved.

**Index Terms**— subsonic wind tunnel, numerical analysis, computational fluid dynamics, calibration, aerodynamics

## I. INTRODUCTION

Subsonic wind tunnel is device used for simulating a characteristic flow over a body. Wind-tunnel testing of full/model-scale components is a frequently used approach for guiding precise design decisions in thermal-fluid systems and enabling basic study into fluid phenomena. The Subsonic Wind Tunnel is the most cost existent setup to provide all-inclusive experimental capabilities in aerodynamics. By utilizing appropriate demonstrative techniques, we can properly understand and enhance the performance of the aircraft. The wind tunnel gives accurate results regarding flow over the body and the aerodynamic forces acting over the body. Investigative methods leading to quantitative forecasting have been a combination of experiment and theory, with numerical methods becoming a new powerful tool. However, experimental explorations remain the mainstay for obtaining data to designers to achieve detailed results and final conclusion across a broad range of industrial and academic applications.

Atmospheric air enters the wind tunnel through an aerodynamically designed inlet which has honeycomb structure and contraction area that accelerates the air in linear manner. Accelerated air then enters the test section and advances through a framework of metal bars before passing through a diffuser and then to a variable-speed axial fan. The framework of metal bars forms a grille which protects the fan from damage by free slack particles. The air leaves the fan, moves through a muffler unit and then back out to atmosphere.

Commonly a freestanding control and instrumentation unit controls the air velocity in the test section and provides electrical power to other instruments.

The test area of the tunnel is a brick section with a lucid roof, sides and floor. The sides are removable. The floor and each side panel have a special emplacement to support wind tunnel models.

Two Pitot-static tubes are provided with the wind tunnel. One is fixed near to the inlet

of the test section and quantifies the air-flow rate. The second Pitot-static tube is connected to a two-axis traverse that allows movement horizontally (fore to aft) and vertically (top to bottom), for measurements throughout the test section.

This paper aims to describe design of subsonic open wind tunnel and development of numerical analysis of flow through the wind tunnel. The wind tunnel is designed to achieve air velocity of approximately 0.8 Mach in the test section. This paper covers the numerical simulation of air flow under experimental conditions with various inlet velocities at the inlet of the wind tunnel which would provide the possibility of calibrating the test section for uniform steady flow.

For the purpose of achieving accurate result using numerical simulation to solve governing equations it is necessary to define adequate meshing and solving technique that can provide good compatibility with both quantitative and qualitative experimental data.

Numerical calculations were done using computational fluid dynamics using realizable K-epsilon turbulence model where the flow features include strong streamline curvature, vortices, and rotation.

Numerical results have also provided in-depth qualitative analysis of flow-field characteristics which are not possible in experimental methods.

## II. DESIGN OF WIND TUNNEL

### A. Wind tunnel design requirements

Proper consideration needs to be exercised when examining characters of low turbulence intensity, flow control and uniformity of the flow inside the wind tunnel as well as cost requirements, fabricating process and future potential developments in the device.

The main factors for this particular wind tunnel were to operate subsonic at Mach 0.8 for research and educational purposes, with passive flow control. The design principles have been established to facilitate accurate measurements of steady or unsteady flow with low turbulence intensity to help the study of the physical phenomena of interest.

Fig. 1 shows a schematic view of the subsonic open wind tunnel designed and its parts (sections) with dimensions.

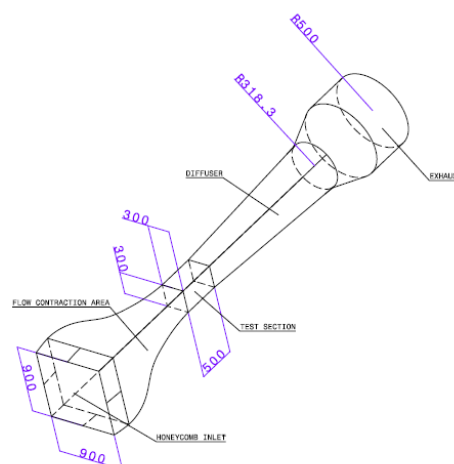


Fig. 1. Diagrammatic representation of subsonic wind tunnel with dimensions

### B. Honey comb inlet

Notwithstanding the challenges imposed by the large size of the flow contraction area

(900×900mm), a set of honeycombs and screens has been consolidated in the design of the settling chamber. Before entering into the settling chamber there is a large screen to add uniformity into the flow, breaking the dirt which may exist in the incoming stream. The design and sizing of each cell in honeycomb have been carried out to decrease swirl and lateral mean velocity fluctuations with a certain pressure drop.

### *C. Flow Contraction Area*

The flow contraction area has a great significance in ascertaining the flow quality in the test section. According to Derbunivich et al.(1987), the flow contraction area accelerates and regulates the flow into the test section. In addition to these benefits, the contraction section is responsible to expand vortex filaments, which decreases axial but increases lateral turbulent changes, as presented by Tennekes and Lumley (1972). The length of the contraction should be amply short to depreciate boundary-layer growth and production cost but, long enough, to limit large adverse pressure gradients along the wall, originated by streamline curvature, this phenomenon can lead to flow separation.

Mehta and Bradshaw (1979) in their paper have discussed about the design of a flow contraction area is aimed to reach a uniform and steady flow at its outlet, and requires the delay of flow separation. Based on the rules, it has been decided a tradeoff between contraction length and contraction ratio, since as a design choice it has been entrusted in the insertion of a settling chamber like honeycombs before the flow contraction area. In this case, it is expected that a higher contraction ratio could take place without risking the flow uniformity in the test section.

The ratio of flow contraction area in inlet to outlet is decided to be 3:1. The flow contraction area is designed to have a length of 1650mm. The inlet of the flow contraction area follows the honey comb section with the same area and gradually converges to 300×300mm with a bell-shaped curve.

### *D. Test Section*

According to Barlow et al. (1999), the primary step in the configuration of a wind tunnel is to decide the size and shape of the test section. This choice depends on the contemplated uses of the facility intrinsically linked to economic support available to assemble the equipment. The test section of wind tunnel is designed as a brick space with 300×300×500mm in dimension.

### *E. Diffuser*

The pattern of the flow exiting the test section affects the flow field inside the diffuser. The flow properties like orientation, size and wake development from models influence the diffuser inlet flow. The cross-sectional shape of the diffuser is designed such that it gradually changes from a square at inlet to circle at outlet to avoid flow separation. The diffuser exit is designed to have cross-sectional area ratio of 3.5 with a diffuser inlet area and the length of the diffuser is appropriately designed to have inlet height to length ratio of 7.1.

### *F. Exhaust*

The exhaust allows the air to exit through it to the atmosphere. The exhaust is diverging for a length of 500m leading to a constant circular area exhaust designed with a radius of 500m.

## III. THREE-DIMENSIONAL MODEL

A three-dimensional model of flow field of the open circuit subsonic wind tunnel is done

with the help of CATIA v5. Here the flow field domain is extracted from the three-dimensional model for the purpose of analysis. The flow field domain is designed to have the following dimensions for each section of the wind tunnel.

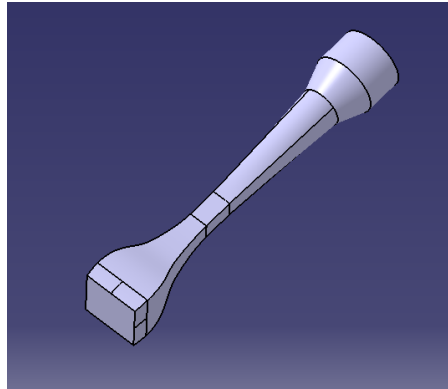


Fig. 2. Three-dimensional domain of the flow field.

TABLE I  
DETAILED DIMENSIONS OF WIND TUNNEL

S. No.	Parameter	Dimensions( mm)
1	Honey comb cross sectional area	900x900
2	contraction inlet area	900x900
3	Flow contraction length	1650
4	Flow contraction outlet area	300x300
5	Test section	300x300x50 0
6	Diffuser length	2130
7	Diffuser exit radius	318.3
8	Exhaust exit radius	500
9	Exhaust length	1100

#### IV. MESHING

Division of the domain into discrete control volumes using a computational grid is known as Meshing. A structured mesh is created with element size of 50mm. Since the structured mesh are aligned in the flow direction, it can lead to more accurate results and better convergence while solving the governing equations using computational fluid dynamics method.

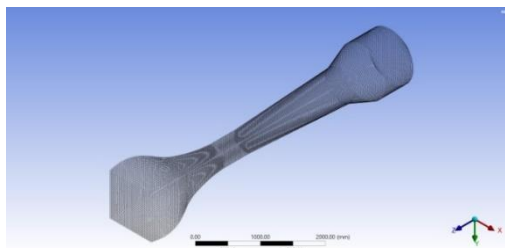


Fig. 3. Structured mesh of domain

The domain is structured mesh since it has arguably higher quality and control and better convergence rate.

TABLE II  
QUALITY OF MESH

S. No.	Parameter	Values
1	Nodes	7920
2	Elements	6390
3	Average aspect ratio	1.8524
4	Average Jacobian ratio	1.2
5	Average Skewness	0.16091

#### V. GOVERNING EQUATIONS

The following governing equations were used to simulate the flow through the wind tunnel:

1. Mass conservation equation
2. Momentum conservation equation
3. Realizable K-epsilon turbulence equation
4. Energy equation

##### A. Mass conservation equation

For any flow, mass conservation equation must be solved. The equation of conservation of mass is given by,

$$\frac{\partial \rho}{\partial t} + \nabla \cdot (\rho \vec{v}) = S_m$$

where

- $S_m$  – the mass added to the continuous phase from the dispersed second phase
- $\rho$  – density of medium (air –  $1.2256 \text{ kg/m}^3$ )
- $v$  – velocity of flow

##### B. Momentum conservation equation

Momentum conservation equation is given by,

$$\frac{\partial}{\partial t} (\rho \vec{v}) + \nabla \cdot (\rho \vec{v} \vec{v}) = -\nabla p + \nabla \cdot (\bar{\tau}) + \rho \vec{g} + \vec{F}$$

where

$p$  – static pressure

$\bar{\tau}$  – stress tensor

$\rho \vec{g}$  – gravitational body forces

$\vec{F}$  – external body forces that arise from synergy with the dispersed phase

The stress tensor  $\bar{\tau}$ , is given by,

$$\bar{\tau} = \mu \left[ (\nabla \vec{v} + \nabla \vec{v}^T) - \frac{2}{3} \nabla \cdot \vec{v} I \right]$$

where

$\mu$  – molecular viscosity

$I$  – unit tensor

$(\nabla\vec{v} + \nabla\vec{v}^T)$  – effect of volume dilation

### C. Realizable K-epsilon turbulence equation

The realizable K-epsilon model is used as it has an improved performance for solving flow involving boundary layers in strong adverse pressure gradients, stream-wise curvature, separation and recirculation zones over the standard K-epsilon model. It also predicts the spreading rates of round jets.

The term "realizable" means that the model satisfies certain mathematical constraints on the Reynolds stresses, consistent with the physics of turbulent flows.

The realizable K-epsilon model is given by,

$$\frac{\partial}{\partial t}(\rho K) + \nabla \cdot (\rho u K) = \nabla \cdot \left[ p \left\{ \frac{v_l + v_t}{\sigma_{t,K}} \right\} \nabla K \right] + \rho(P_K - \varepsilon)$$

$$\frac{\partial}{\partial t}(\rho K) + \nabla \cdot (\rho u \varepsilon) = \nabla \cdot \left[ p \left\{ \frac{v_l + v_t}{\sigma_{t,\varepsilon}} \right\} \nabla \varepsilon \right] + \rho \left( \frac{C_{1\varepsilon} S \varepsilon - C_{2\varepsilon} \varepsilon^2}{\{K + \sqrt{v_l \varepsilon}\}} \right)$$

where

$$v_t = C_\mu \frac{K^2}{\varepsilon}$$

$$P_K = v_t S^2$$

$$S = \sqrt{2S_{ij}^2}$$

$$S_{ij} = 0.5 \left( \frac{\partial u_i}{\partial x_j} + \frac{\partial u_j}{\partial x_i} \right)$$

The model coefficients  $C_{1\varepsilon}$  and  $C_\mu$  are computed from the following equations:

$$C_{1\varepsilon} = \max \left[ 0.43, \frac{\eta}{(\eta+5)} \right]$$

where

$$\eta = \frac{SK}{\varepsilon}$$

$$C_\mu = \frac{1}{\left[ A_0 + A_S K \frac{\hat{U}}{\varepsilon} \right]}$$

where

$$\hat{U} = \sqrt{S_{ij}^2 + \Omega_{ij}^2}$$

$$\Omega_{ij} = 0.5 \left( \frac{\partial u_i}{\partial x_j} - \frac{\partial u_j}{\partial x_i} \right)$$

$$A_S = \sqrt{6 \cos \Phi}$$

$$\Phi = \cos^{-1} [\max(-1, \min[\sqrt{6W}, 1])] ]$$

$$W = \frac{S_{ij} S_{jk} S_{ki}}{\check{S}^3}$$

$$\check{S} = \sqrt{S_{ij}^2}$$

The other empirical constants are given by,

$$\sigma_{t,K} = 1.0$$

$$\sigma_{t,\varepsilon} = 1.2$$

$$A_0 = 4.04$$

$$C_{2\varepsilon} = 1.9$$

#### D. Energy conservation equation

The turbulent heat transfer is modeled using the concept of Reynolds' analogy to turbulent momentum transfer. The governing equation used in modelling the flow is given by,

$$\frac{\partial}{\partial t}(\rho E) + \frac{\partial}{\partial x_i}[u_i(\rho E + p)] = \frac{\partial}{\partial x_j}\left(k_{eff} \frac{\partial T}{\partial x_j} + u_i(\tau_{ij})_{eff}\right) + S_h$$

where

$E$  - total energy

$k_{eff}$  - effective thermal conductivity

$(\tau_{ij})_{eff}$  - deviatoric stress tensor

Stress tensor  $(\tau_{ij})_{eff}$ , is given by,

$$(\tau_{ij})_{eff} = \mu_{eff} \left( \frac{\partial u_j}{\partial x_i} + \frac{\partial u_i}{\partial x_j} \right) - \frac{2}{3} \mu_{eff} \frac{\partial u_k}{\partial x_k} \delta_{ij}$$

Stress tensor equation is solved to include viscous heating.

For realizable k-epsilon model, effective thermal conductivity is given by,

$$k_{eff} = k + \frac{c_p \mu_t}{Pr_t}$$

where

$k$  - thermal conductivity

$Pr_t$  - Prantl number(0.85)

## VI. NUMERICAL ANALYSIS

### A. Boundary Conditions

Since the purpose of this paper is to calibrate test section of subsonic wind tunnel, various inlet velocities ranging from 5m/s to 30m/s with constant total pressure of 101325 Pa and temperature of 303 K are considered.

TABLE III

BOUNDARY CONDITIONS

Case No.	1	2	3	4	5	6
Velocity (m/s)	5	10	15	20	25	30

### B. Methods used to achieve solve Governing equations

The methods used to solve the governing equations by numerical analysis to simulate the flow in the subsonic wind tunnel are as follows. Pressure based solver is used here since the flow is subsonic and incompressible. In pressure-based solver velocity field is obtained by solving the momentum equations. The pressure field is obtained by solving pressure correction equation which is obtained by manipulating continuity and momentum equations. ANSYS FLUENT solves the governing integral equations for the conservation of mass, momentum, energy and turbulence. A control-volume-based technique is used that consists of:

- Integration of the governing equations on the individual control volumes to construct algebraic equations for the discrete dependent variables such as velocities, pressure, temperature, and conserved scalars.
- Linearization of the discretized equations and solution of the resultant linear equation system to generate updated values of the dependent variables.

The pressure-based coupled solver uses a solution algorithm where the governing equations are solved simultaneously. Because the governing equations are non-linear and coupled, the solution loop must be carried out iteratively to achieve a converged numerical solution.

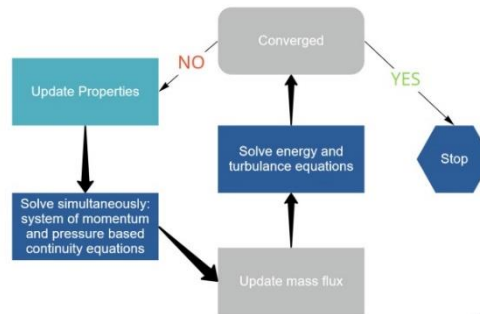


Fig. 4. Step to solve governing equations by Pressure based coupled solver

To delineate and calculate the values of scalar quantities like turbulent kinetic energy, turbulent dissipation rate and enthalpy at the cell faces, secondary diffusion terms and velocity derivatives gradients are needed. The gradient of the given scalar variable is used to discretize the convection and diffusion distinct quantities in each governing equation. The solution is assumed to vary linearly and linear systems of governing equations are over-determined and results are achieved by breaking down the coefficient matrix by Gram-Schmidt procedure. Second order spatial discretization is desired for solving pressure, momentum, two turbulent and energy equations so that the quantities are calculated at the cell faces using a multidimensional linear approach. Higher order accuracy is accomplished at the faces of each cell through Taylor series expansion of cell centered solution about the centroid of cell. Solution is initialized by hybrid method for 15 numbers of iterations to achieve a convergence tolerance of micron level. Then the calculation is done using iterative method till the solution is converged.

## VII. RESULTS AND DISCUSSIONS

Once the solution is converged, post-processing of the results depicting velocity contours, static pressure contours, temperature contours are done.

### A. Velocity contours of flow through wind tunnel

Velocity contours showing magnitude of velocity of flow stream by measuring the elemental areas between consecutive isovels and summing the products of a specific area by the average of its boundary velocities is plotted. The velocity contour show in all the considered cases the velocity of the flow is increasing at the flow contraction area of the wind tunnel and then when the air enters the test section the velocity kept on creasing and reaches a maximum. After the test section the velocity decreases as the downstream of the diffusion section of the wind tunnel.



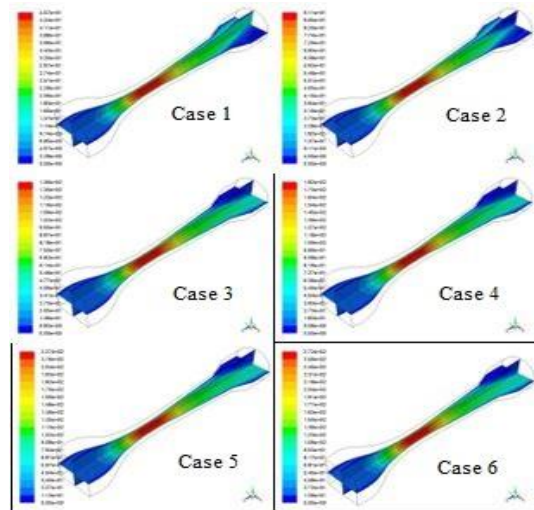


Fig. 5. Velocity contours of flow in the wind tunnel

*B. Total temperature contours at test section of wind tunnel*

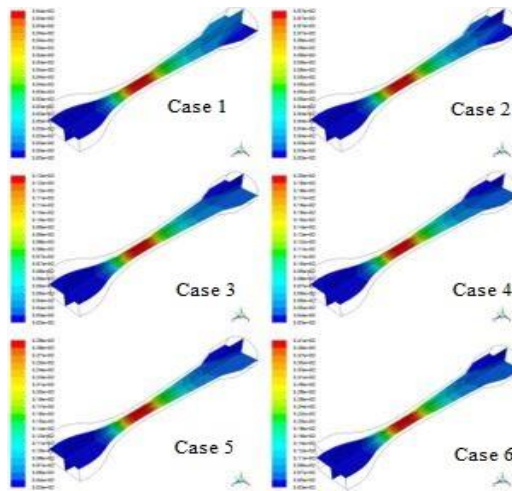


Fig. 6. Total temperature contours of flow in the wind tunnel

Total temperature contour showing flow temperature is plotted. It is detected from the total temperature contour that the flow is having high temperature at the test section. As the air enters the flow contraction area, flow temperature witnesses a steady increase. When the reaches test section the flow temperature reaches a maximum and at the diffusion section the flow temperature diminishes progressively. The maximum temperature at the test section indicates that the molecules of air are very closer to each other and attempting to escape the test section coercively through the diffuser section where the pressure gradient is weaker compared to the flow contraction area.

*C. Static pressure contours at test section of wind tunnel*

Static pressure contour showing the flow pressure in is plotted. It is observed from the static pressure contour that the flow is having high pressure at the settling chamber. As the air enters the flow contraction area, flow pressure decreases gradually. When the air reaches test section the flow pressure reaches a minimum and at the diffusion section the flow pressure increases gradually. The flow is not reversing from the test section to the flow contraction area since the pressure gradient is higher than the diffusion section of the wind tunnel.

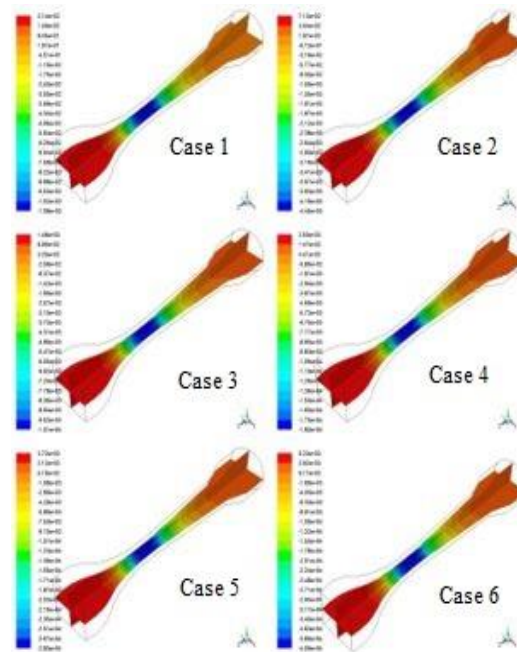


Fig. 7. Static pressure contours of flow in the wind tunnel

#### D. Velocity contours at test section of wind tunnel

When the velocity contours of the flow at the test section are examined, they showed that the velocity is maximum at the centre of the test section and the flow velocity is decreased at upstream and downstream of the centre section of the test section.

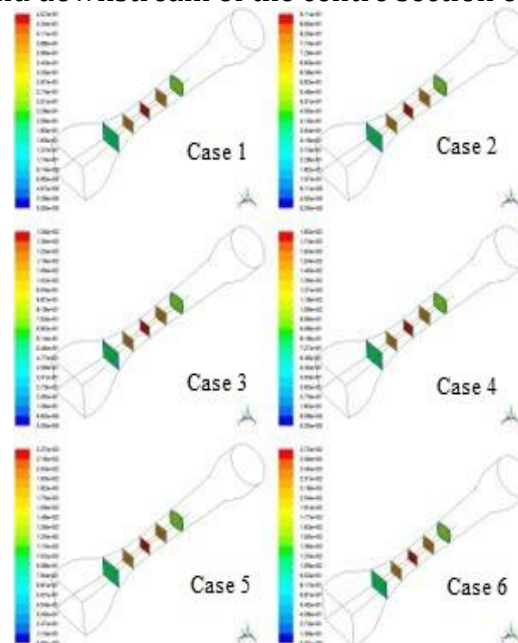


Fig. 8. Velocity contours of flow at the test section of the wind tunnel

#### E. Comparison of Velocity magnitude at the test section for all cases

The velocity at the centre plane of the test section is further analysed and the velocity according to the vertical position is plotted. The centre of the flow is having maximum velocity and towards the wall there is reduced velocity.

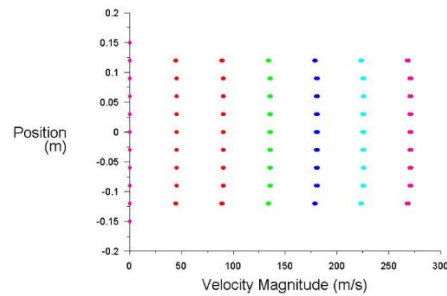


Fig. 9. Comparison of velocity at center plane of test section of the wind tunnel

TABLE IV

AVERAGE VELOCITY AT CENTER OF TEST SECTION

Case No.	Inlet velocity $\left(\frac{m}{s}\right)$	Average value of Velocity at Center of test section $\left(\frac{m}{s}\right)$
1	5	45.00
2	10	89.99
3	15	134.99
4	20	179.99
5	25	224.98
6	30	269.98

#### VIII. CONCLUSION

The subsonic wind tunnel is designed and calibrated for the flow through the test section by utilizing numerical calculations involving solving equations that govern the aspects of flow.

The design for the subsonic wind tunnel is created and the design considerations were prolific for flow conditions up to Mach 0.8. The flow is simulated for various inlet velocity conditions and shows very robust results in this study. The solution methodologies to solve the governing equations are found to be giving sufficient reliable results.

According to these predictions of velocity, pressure and temperature the design for the subsonic wind tunnel is having capacity of handling Mach 0.8 at the test section.

#### REFERENCES

- [1] Derbunivich, G.I., Zemskaya, A.S., Repik, E.U. and Sosedko, Y.P.(1987) Effect of flow contraction on the level of turbulence. *Izv.Akad. Nauk SSSR Mekh. Zhidk. Gaza*, 2, 146–152.
- [2] J. K. Calautit, B. R. Hughes, “CFD and experimental data of closed-loop wind tunnel flow”, *Data in Brief*, Volume 7, 2016, Pages 216-220, ISSN 2352-3409, <https://doi.org/10.1016/j.dib.2016.02.033>
- [3] Nedyalkov, Ivaylo, “Design of Contraction, Test Section, and Diffuser for a High-Speed Water Tunnel”. Master’s thesis, Chalmers University of Technology, Gothenburg, Sweden, 2012.
- [4] J. K. Calautit, H. N. Chaudhry, B. R. Hughes, L. F. Sim, “A validated design methodology for a closed-loop subsonic wind tunnel”, *J. Wind Eng.Ind.Aerodyn.*125(2014)180–194.
- [5] Tennekes, H. and Lumley, J.L. (1972) *A First Course in Turbulence*, MIT Press, Cambridge, Massachusetts.

- 
- [6] M. A. Moelyadi, M. F. Izzaturrahman, C. Adnel, M. H. Izzuddin, and E. Amalia, "Design and CFD simulation of a compact supersonic wind tunnel", AIP Conference Proceedings 2226, 020009 (2020) <https://doi.org/10.1063/5.0003727>
- [7] Pope A. and Goin K. L., High Speed Wind Tunnel Testing, John Wiley & Sons, 1965.
- [8] Ibrahim M. K., Abohelwa, A. F., dan Salem G. B. 2009, "Design, fabrication, and realization of a supersonic wind tunnel for educational," in International Journal of Mechanical Engineering Education, Vol. 37, No. 4, 286–303. <https://doi.org/10.7227/IJMEE.37.4.3>
- [9] P. Sofotasiou, J. K. Calautit, B. R. Hughes, D. O'Connor, "Towards an integrated computational method to determine internal spaces for optimum environmental conditions", *Comput. Fluids* (2016), <http://dx.doi.org/10.1016/j.compfluid.2015.12.015>.
- [10] T. Studd, "CFD & wind tunnels reverse roles," R&D Magazine, vol. 46, no. 3, pp. 19–21, March 2004.
- [11] J. H. Bell and R. D. Mehta, "Contraction design for small low-speed wind tunnels," NASA STI/Recon Technical Report N, vol. 89, p. 13753, Aug. 1988
- [12] Le, Hong-Hieu & Nguyen, Chi-Cong & Le, Khoi & Bui, Dat & Nguyen, Ngoc-Hien. (2015). Integrated design process for Subsonic Open Circuit Wind Tunnel from empirical studies to CFD simulation. 10.1109/ATC.2015.7388426.
- [13] Javed, Kashif & Professor, Assistant & Ali, Mazhar. (2014). Design & Construction of subsonic wind Tunnel focusing on two dimensional contraction cone profile using sixth order polynomial (Design of Subsonic Wind Tunnel Contraction cone profile through CFD Simulation).
- [14] Bradshaw, P. and Mehta, R. Wind Tunnel Design, <http://www-htgl.stanford.edu/bradshaw/tunnel/> (accessed 18 June 2009).
- [15] M. Abbaspour & M.N Shojaee: "Innovative approach to design a new national low speed wind tunnel", Department of Mechanical Engineering, Sharif University of Technology and Graduate School of the Environment & Energy, Science and Research branch IAU, Tehran, Iran, 10 Dec. 2008.
- [16] Barlow JB, Rae Jr WH, Pope A (1999) Low-speed wind tunnel testing. 3rd edition. New York: John Wiley and Sons.
- [17] Almeida O; Miranda FC; Ferreira Neto O; Saad FG (2018). Low Subsonic Wind Tunnel – Design and Construction. *J Aerosp Technol Manag*, 10: e1018. doi: 10.5028/jatm.v10.716.
- [18] Derbunivich GI, Zenskaya AS, Repik EU, Sosedko YP (1987) Effect of flow contraction on the level of turbulence. *Fluid Dynam* 22(2):289-294. doi: 10.1007/BF01052265
- [19] Su Y (1991) Flow analysis & design of three-dimensional wind tunnel contractions. *AIAA J* 29(11):1912-1920.